EUROPEAN ORGANIZATION FOR NUCLEAR RESEARCH
European Laboratory for Particle Physics

Large Hadron Collider Project

LHC Project Report 377

Tune Scan Studies for the LHC at Injection Energy

L. Jin, IHEP, Beijing, on leave of absence

and

F. Schmidt, CERN

Abstract

The choice of a working point in the betatron tune diagram is very important for the design of a collider like the LHC: to a great extent the performance of the collider depends on the working point. To understand the dependence of the dynamic aperture on the choice of the working point in the LHC, a thorough tune scan by particle tracking in the six dimensional phase space has been performed for several LHC models at the injection energy over a wide tune range and for different values of the distance from the tune diagonal ($Q_x - Q_y = 0.03$) in order to find optimal fractional betatron tunes. The results of the tune scan are discussed and analysed in this report.

Administrative Secretariat
LHC Division
CERN
CH-1211 Geneva 23
Switzerland

Geneva, 22 May 2000

1 Introduction

In Ref. [1], a tune scan has been performed at three different distances ($Q_x - Q_y = -0.01$, $Q_x - Q_y = -0.03$, $Q_x - Q_y = -0.05$) from the tune diagonal over a wide tune range for the optics version 5 of the LHC with the *target error table* [2] (see Appendix A) at the injection energy. Although it seems there is more space available between low order resonances for the case of $Q_x - Q_y = -0.01$ than for $Q_x - Q_y = -0.03$, the former case doesn't show any improvement of the long–term dynamic aperture. In fact, for instance the dynamic apertures at $(Q_x, Q_y) = (0.27, 0.28)$ have been confirmed by long–term tracking (100,000 turns) to be significantly smaller than for $(Q_x, Q_y) = (0.27, 0.30)$. For the case of $Q_x - Q_y = -0.05$, more resonances play a role and the islands of particle stability become much smaller. Figure 1 shows the tracking results for the case of $Q_x - Q_y = -0.03$, on which the nominal working point (0.28,0.31) lies. From the study of Ref. [1], an optimal fractional working point was found at (0.27,0.30) which shows the largest dynamic aperture.

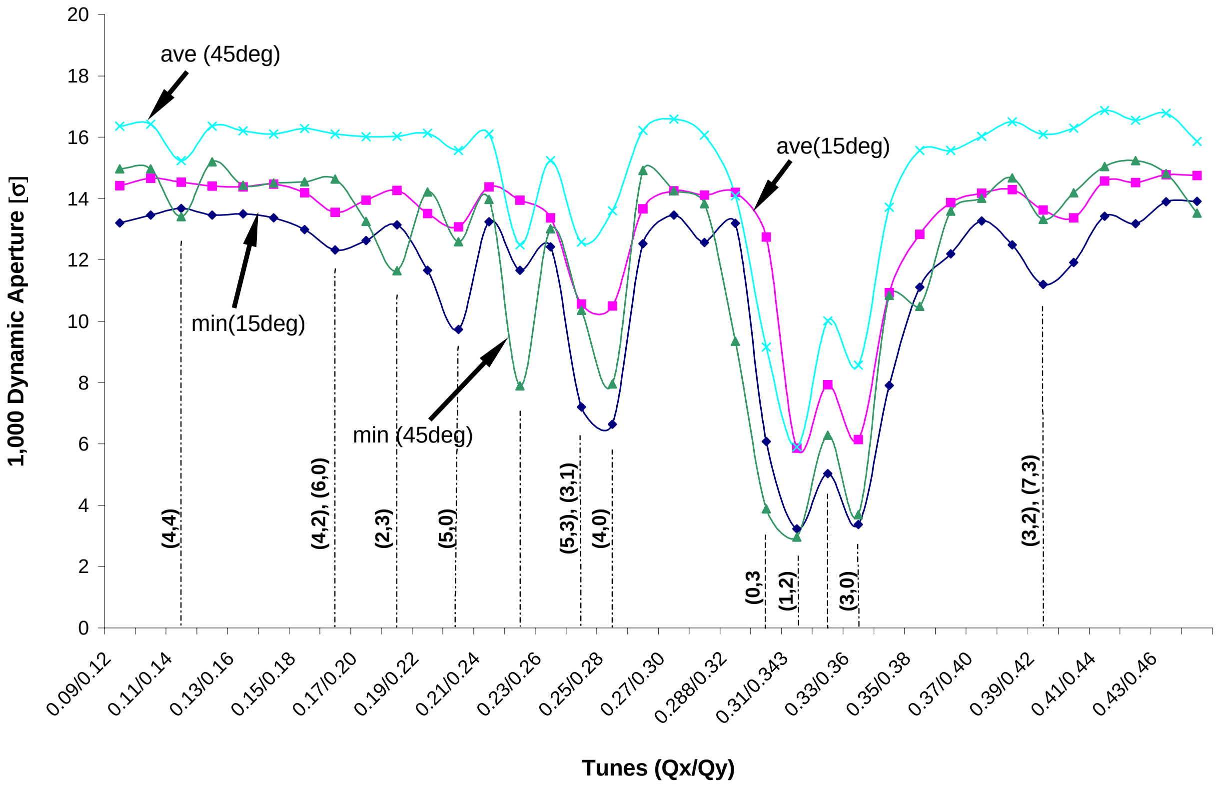

Figure 1: Short–term dynamic aperture (1,000 turns) v.s. tune for the LHC optics version 5 with the *target error table*. Average and minimum value over 60 random seeds are given at the phase space angles $\phi = 15°, 45°$ respectively for each pair of tunes, which are separated by 0.03.

Each entry in the Figure 1 is the result of a tracking run over 1,000 turns for 60 different random realizations of the multipole errors, called random seeds in the following. The dynamic aperture is expressed in terms of the transverse r.m.s. beam size σ, the LHC normalised emittance is 3.75μm at 1σ. Particle motion samples different resonances depending on the ratio between horizontal and vertical oscillation amplitudes, with

$$A_x = \sqrt{\beta_x \cdot \epsilon_x}; A_y = \sqrt{\beta_x \cdot \epsilon_y} \tag{1}$$

with ϵ_x, ϵ_y the horizontal and vertical transverse emittances, respectively. To obtain a realistic estimate for the dynamic aperture one has to vary this ratio, expressed as a phase space angle:

$$\phi = \arctan\left(\sqrt{\frac{\epsilon_y}{\epsilon_x}}\right). \tag{2}$$

As a bare minimum one has to study round beams (equal horizontal and vertical emittance) and the case of mainly horizontal motion (horizontal emittance much larger than the vertical emittance). The tracking is performed in the full six–dimensional phase space at 75% of the bucket half size, (i.e. ($\frac{\delta p}{p_0} = 0.00075$) using the tracking code SixTrack [3]. The amplitude has been varied in steps of $\frac{1}{15}\sigma$ to determine the minimum and average dynamic aperture for the 60 random seeds. It is necessary to use two values for the dynamic aperture since the minimum is a possible worst case, with a 95% probability that the true dynamic aperture is above this value, and the average dynamic aperture serves to compare the overall quality of the different lattices. The uncertainty of the minimum value is about 0.5σ while it is some 0.2σ for the average dynamic aperture.

Following the study in Ref. [1], this report presents the results of tune scans for the LHC nominal optics version 6 with the recent realistic error table **9901** (see Appendix A) and the "resonance–free" lattice [4, 5] with the same error table. Linear imperfections are not included in all these studies, which may explain the large dynamic aperture for small tunes say below (0.15,0.18). In addition, more analyses have been made to understand why the working point (0.27,0.30) shows a larger dynamic aperture than the nominal working point (0.28,0.31). The total tune range studied is 0.35 in both planes, and the tune is varied in steps of 0.01 using the QF and QD quadrupoles in the normal cells of the arcs and the dispersion suppressors.

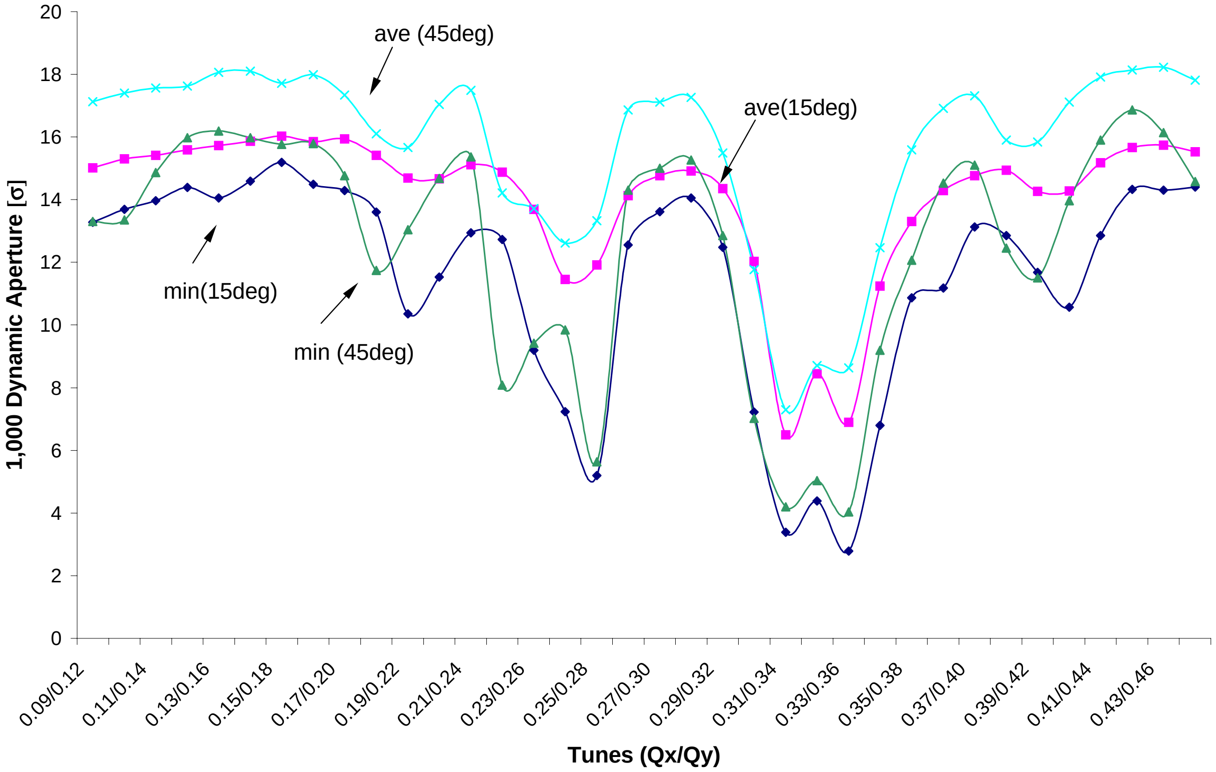

Figure 2: Short–term dynamic aperture (1,000 turns) v.s. tune for the LHC optics version 6 with the error table **9901**. Average and minimum value over 60 random seeds are given at the phase space angles $\phi = 15°, 45°$ respectively for each pair of tunes, which are separated by 0.03.

The maximum beta beating in the explored tune range is about 7%. Besides short–term tracking (1,000 turns) some cases are tracked for 100,000 turns to check their long–term behaviour.

The paper is organised as follows: the tracking for the nominal LHC version 6 together with a thorough resonance analysis is presented in section 2. A discussion of the tracking studies for the "resonance–free" lattice and the comparison with the nominal case follows in section 3. This last section first treats the 4^{th} order, then the 3^{rd} order resonances and finally it discusses long–term tracking results.

2 Results for LHC Optics Version 6 and their Analysis

The LHC optics version 6 [6] is the recently optimised optics in which the integer tune split is 5 instead of 4, as used in the optics version 5. The tracking is performed with the error table **9901** and the resulting scan is shown in Figure 2. Globally the resonance structure presents a similar pattern to what we obtained for the optics version 5 (see Figure 1).

The main stability islands are separated by the 3^{rd} and 4^{th} order resonances. The three good regions with large dynamic aperture are located around working points (0.15,0.18), (0.28,0.31) and (0.42,0.45) respectively. The dynamic apertures determined by long–term tracking (100,000 turns) around these three working points are listed in Table 1 for both the optics version 5 with the *target error table* and the optics version 6 with the error table **9901**.

Working Point Q_x/Q_y		**Dynamic Aperture (100,000 turn)**			
		$\phi = 15°$		$\phi = 45°$	
		Minimum	**Average**	**Minimum**	**Average**
Version 5 with the target error table	0.28/0.31	11.3	12.4	12.3	13.8
	0.27/0.30	**12.2**	**12.7**	**13.1**	**14.2**
	0.14/0.17	11.7	12.6	12.6	14.2
	0.15/0.18	11.8	12.9	11.3	14.2
	0.42/0.45	11.7	12.9	11.2	14.0
Version 6 with the error table 9901	0.28/0.31	11.5	12.9	11.8	14.4
	0.27/0.30	**11.7**	**13.2**	**12.5**	**14.4**
	0.14/0.17	12.0	13.5	12.2	14.7
	0.15/0.18	11.9	13.6	12.7	15.0
	0.42/0.45	11.6	13.4	12.4	14.7

Table 1: Long–term dynamic aperture at some specific working points which are located around the three stability islands of the global tune scan pictures (see Figure 1 and Figure 2). Average and minimum value over 60 random seeds are given at the phase space angles $\phi = 15°, 45°$ respectively for each working point.

It is noticeable from Table 1 that the average dynamic apertures for the optics version 6 at all those working points are about 0.2 to 0.9 σ larger than for the optics version 5 even though a more realistic error table is used. This indicates that the optics version 6 is indeed favourable and gives globally a larger dynamic aperture than the optics version 5.

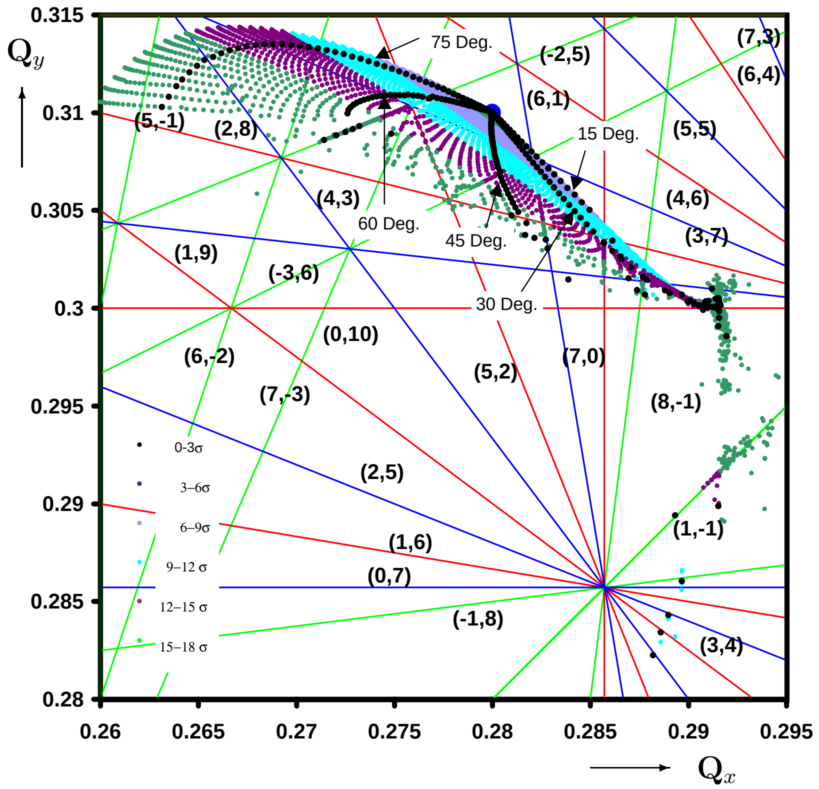

Figure 3: Frequency map (*random seed 24*) for the LHC optics version 6 with the error table **9901**. Particle amplitude varies from 0 to 18 σ in steps of 0.3 σ and phase space angles from 0 to $\pi/2$ in steps of $\pi/204$, each point representing one different orbit in the frequency map. The darkest black dots denote particles with phase space angles of $15°$, $30°$, $45°$, $60°$ and $75°$. The tune footprint is determined by particle tracking over 1,000 turns and subsequent analysis à la Laskar [7, 8]. Some resonance lines are included and identified by labels.

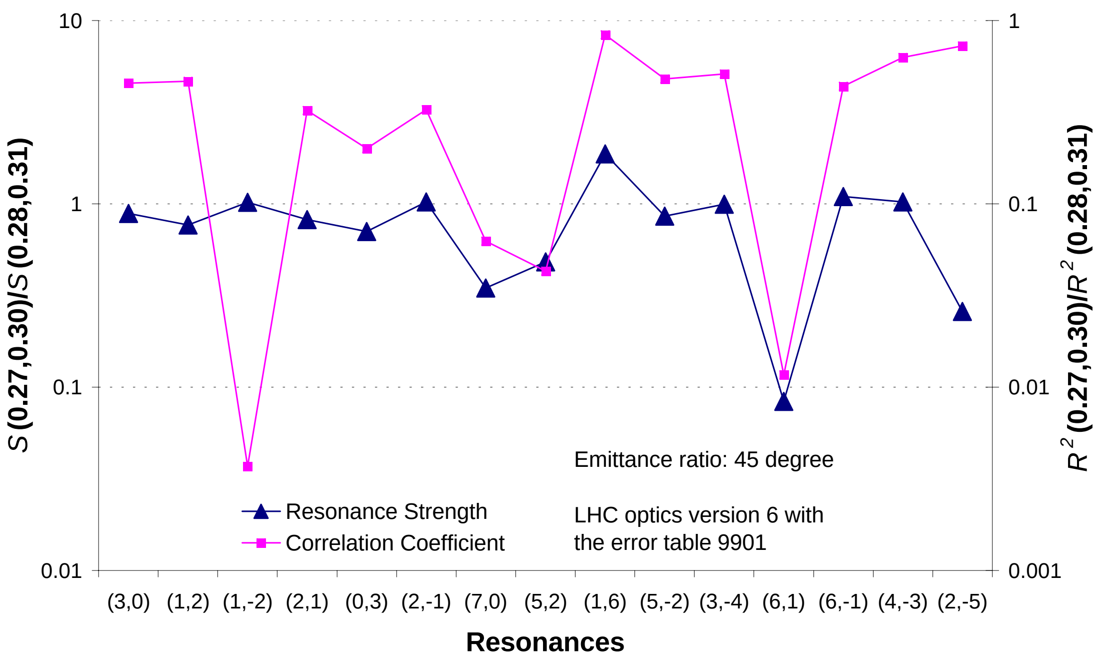

Figure 4: Ratio of the resonance strengths and correlation coefficients between working point (0.27,0.30) and (0.28,0.31) at the phase space angle $\phi = 45°$ for some important resonances. S: Average value of the resonance strength over 60 random seeds at 8σ and up to 12^{th} order; R^2: Average correlation coefficient between dynamic aperture and resonance strength.

Consistently with the conclusion from Ref. [1], the working point (0.27,0.30) indeed shows a larger dynamic aperture than the nominal working point also for the optics version 6 with the error table **9901**. A frequency map for the worst *random seed 24* has been completed at the nominal working point as shown in Figure 3. As for the optics version 5 (see Ref. [8]), the same 7^{th} order resonances such as (7,0),(6,1),(–2,5) and (5,2) lead to strong deformations as seen in the frequency map. We therefore expect that they have an impact on the dynamic aperture.

<table>
<tr><th rowspan="3">Resonance</th><th colspan="6">Correlation Coefficient R^2</th></tr>
<tr><th colspan="2">For single resonance</th><th colspan="2">Combination I</th><th colspan="2">Combination II</th></tr>
<tr><th>(0.28, 0.31)</th><th>(0.27, 0.30)</th><th>(0.28, 0.31)</th><th>(0.27, 0.30)</th><th>(0.28, 0.31)</th><th>(0.27, 0.30)</th></tr>
<tr><td>(3,0)</td><td>0.057</td><td>0.026</td><td rowspan="6">0.230</td><td rowspan="6">0.067</td><td rowspan="15">0.532</td><td rowspan="15">0.220</td></tr>
<tr><td>(1,2)</td><td>0.015</td><td>0.007</td></tr>
<tr><td>(1,-2)</td><td>0.0189</td><td>0.00007</td></tr>
<tr><td>(2,1)</td><td>0.034</td><td>0.011</td></tr>
<tr><td>(0,3)</td><td>0.045</td><td>0.009</td></tr>
<tr><td>(2,-1)</td><td>0.046</td><td>0.015</td></tr>
<tr><td>(7,0)</td><td>0.016</td><td>0.001</td><td rowspan="9">0.413</td><td rowspan="9">0.178</td></tr>
<tr><td>(5,2)</td><td>0.093</td><td>0.004</td></tr>
<tr><td>(1,6)</td><td>0.037</td><td>0.031</td></tr>
<tr><td>(5,-2)</td><td>0.129</td><td>0.062</td></tr>
<tr><td>(3,-4)</td><td>0.0745</td><td>0.038</td></tr>
<tr><td>(6,1)</td><td>0.016</td><td>0.0002</td></tr>
<tr><td>(6,-1)</td><td>0.057</td><td>0.025</td></tr>
<tr><td>(4,-3)</td><td>0.081</td><td>0.051</td></tr>
<tr><td>(2,-5)</td><td>0.092</td><td>0.067</td></tr>
</table>

Table 2: Comparison of the average correlation coefficients between dynamic aperture and resonance strengths for the nominal working point (0.28,0.31) and the working point (0.27,0.30) for the phase space angle $\phi = 45°$. 60 random seeds are taken into account for this study and resonance strengths are calculated at 8σ and up to 12^{th} order with the code GRR. Combination I indicates the combination of either 3^{rd} or 7^{th} order resonances while in Combination II all resonances are combined.

More detailed studies showed that the 7^{th} and 3^{rd} order resonances have a quite important effect on dynamic aperture at the nominal working point. The code GRR [9] was used to evaluate the strength of the resonances up to a given order. These resonance terms are provided by a Normal Form analysis of one–turn maps via the Dalie Code [10]. Then, the LINEST function of EXCEL was used to do linear multi–variant fits for the correlation between the dynamic aperture and the combination of several resonance strengths.

Table 2, shows that the combination of all resonances (combination II) via a linear multi–variant fit results in a correlation coefficient $R^2 = 0.53$ at the nominal working point while at the working point (0.27,0.30) the correlation coefficient is reduced to $R^2 = 0.22$. This means that the correlation coefficient is inversely proportional to the dynamic aperture.

Notice that the correlation coefficients for every single resonance (see Table 2) show the benefit of the working point (0.27,0.30) compared with the nominal working point. Lastly, one finds that the 7^{th} order resonances are relatively more dangerous than resonances of 3^{th} order and that the correlation is slowly increasing when more and more resonances are included (compare combination I and II respectively in Table 2). This confirms the well known fact that the dynamic aperture at a tune working point far from single low order resonances is determined by many weakly excited resonances.

Figure 4 further indicates the advantage of the working point (0.27,0.30) as most of the those resonances (especially some 7^{th} order resonances) become weaker compared with the case of the nominal working point. At the same time the reduction of the correlation coefficient R^2 for the working point (0.27,0.30) is shown.

3 Tracking Results for the "Resonance–Free" Lattice

A "resonance–free" lattice with a tune split of 9 has been proposed [4,5] in which most of the low order resonance driving terms excited by the mean and systematic per arc (uncertainty) multipole errors can be suppressed to first order automatically, arc by arc, through setting the cell phase advances in both planes to satisfy certain conditions.

With the error table **9901**, a tune scan has been performed for this lattice (see Figure 5 part a.). Compared with the nominal optics version 6, the lattice apparently shows some improvement for dynamic aperture globally in the three stability islands and long–term tracking for some working points in the stability islands also confirm this fact (see Table 3).

Working Point Q_x/Q_y	**Dynamic Aperture (100,000 turn)**			
	$\phi = 15°$		$\phi = 45°$	
	Minimum	**Average**	**Minimum**	**Average**
0.28/0.31	11.8	13.5	13.5	15.3
0.27/0.30	11.6	**13.9**	13.2	**15.8**
0.15/0.18	11.7	14.2	13.4	15.9
0.42/0.45	10.2	13.5	11.6	15.4

Table 3: Long–term dynamic aperture at some specific working points which are in the three stability islands of the global tune–scan picture for the "resonance–free" lattice with the error table **9901**. To see the dynamic aperture improvement, compare it with the Table 1. Average and minimum value over 60 random seeds are given at the phase space angles $\phi = 15°, 45°$ respectively for each working point.

It should be noted that the working point (0.27,0.30) shows a slightly larger dynamic aperture in average than the nominal working point (0.28,0.31) for the "resonance–free" lattice as well (see Table 3). But unfortunately the cancellation of the resonances doesn't seem as effective as foreseen, and the dangerous 3^{rd} and 4^{th} order resonances still appear in the picture of the tune scan.

a.)

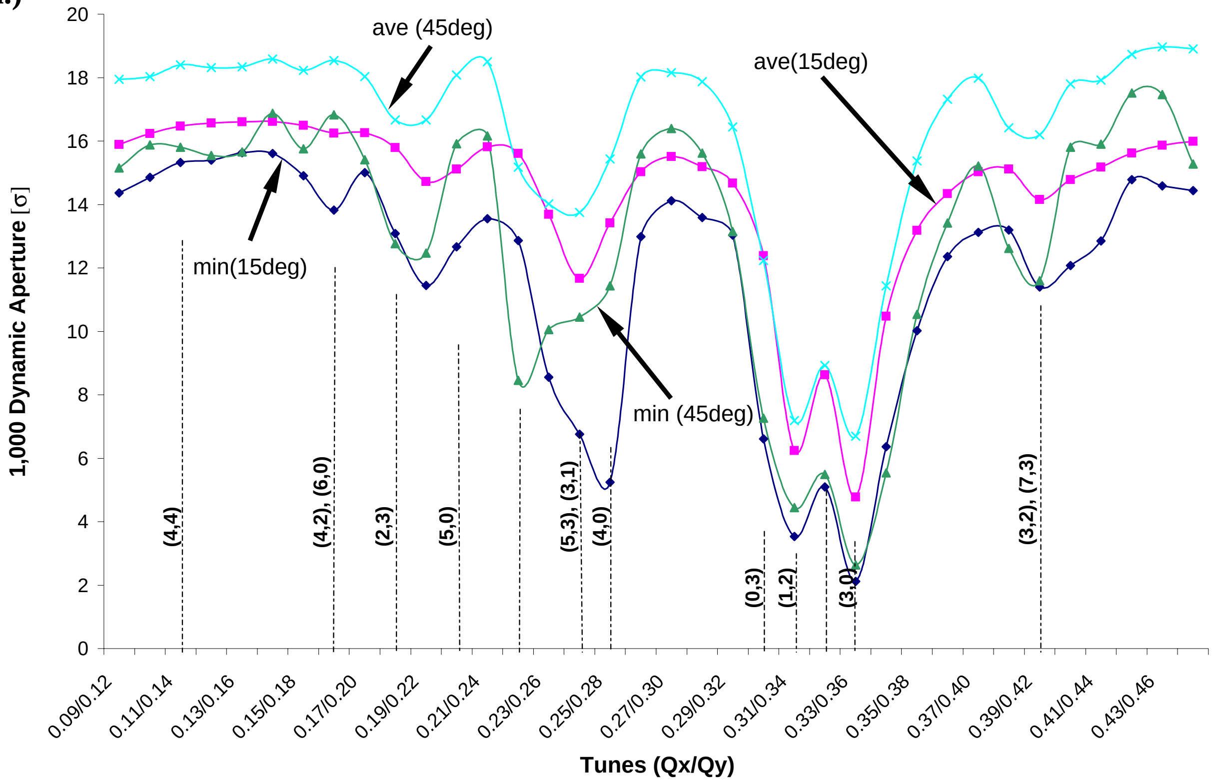

b.)

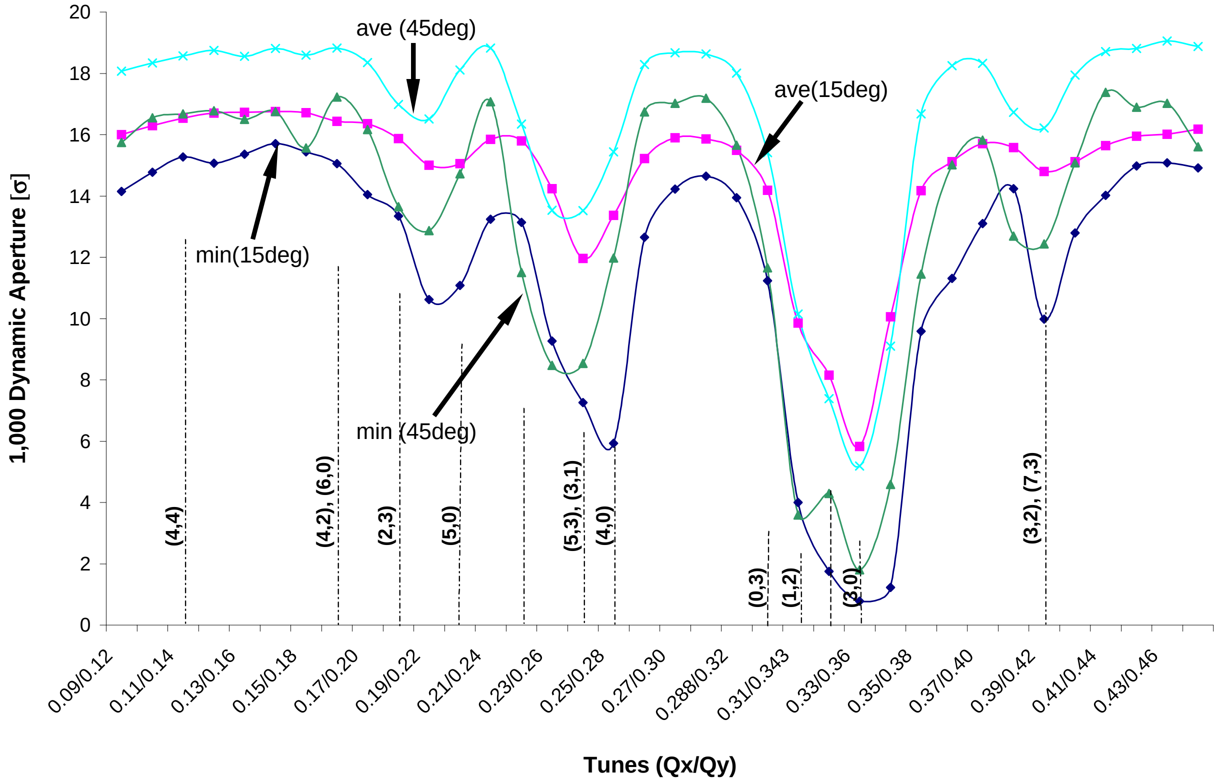

Figure 5: Short–term dynamic aperture (1,000 turns) v.s. tune for the LHC “resonance–free” lattice with the error table **9901**. Average and minimum value over 60 random seeds are given at the phase space angles $\phi = 15^\circ, 45^\circ$ respectively for each pair of tunes, which are separated by 0.03.
Part **a)**: Nominal number of chromaticity sextupoles;
Part **b)**: Additional chromaticity sextupoles in the D.S. (see Sect. 3.3).

3.1 4^{th} Order Resonances

To understand what is happening for the 4^{th} order resonances, the code SODD [11] was used to calculate the resonance driving terms produced by b_4 at the nominal working point for both the “resonance–free” lattice and the nominal optics version 6. The *random seed 2* was taken as an example. Figure 6 **a)** shows indeed that in the “resonance–free” lattice half of the driving terms from b_4 (mean and uncertainty) become much smaller than in the case of the nominal optics version 6. [1)]

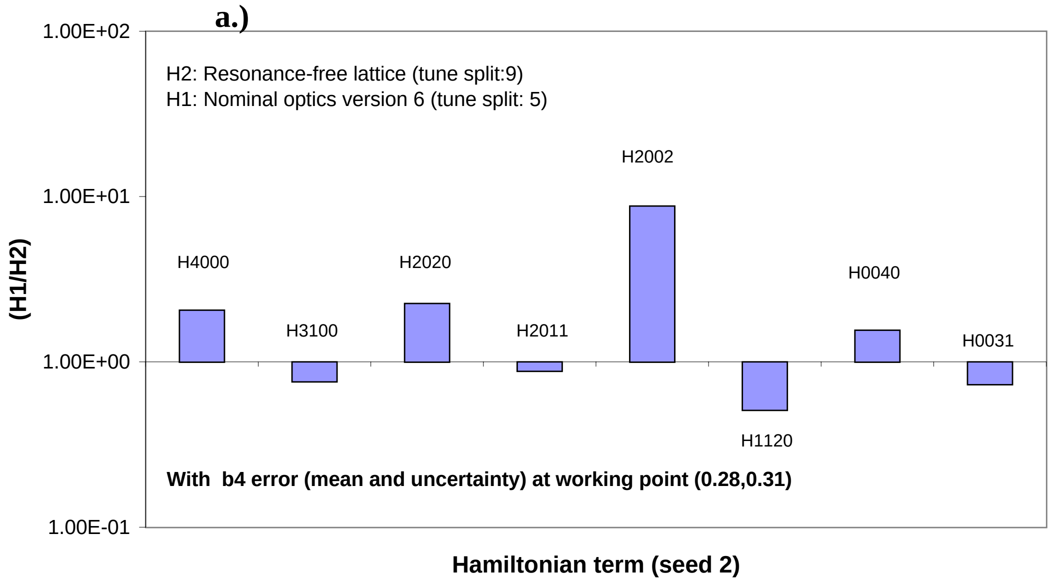

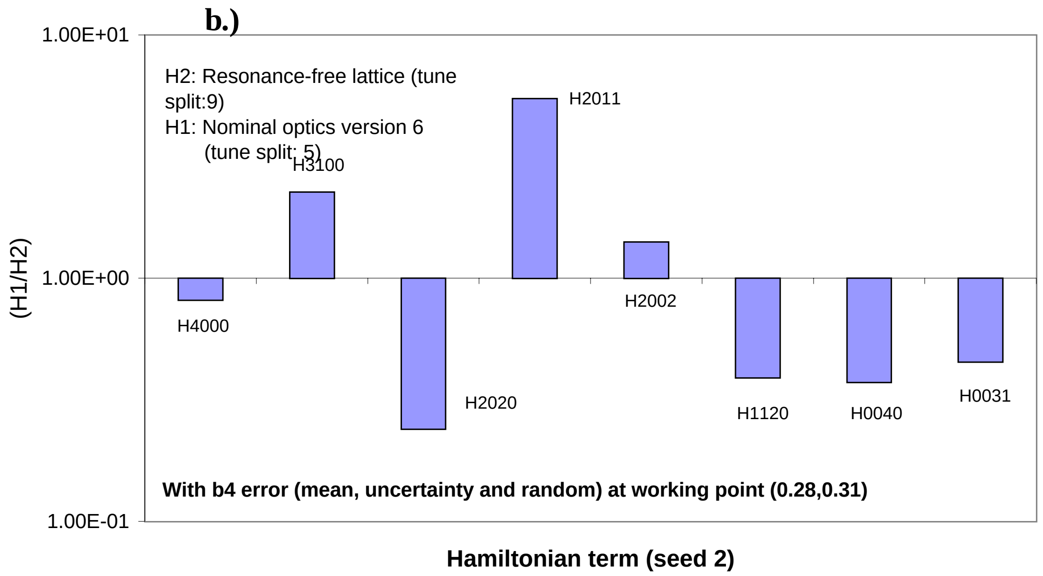

Figure 6: Ration between Hamiltonian terms driven by multipole b_4 for the nominal optics version 6 and the “resonance–free” lattice. The labels on the bars indicate the type of resonance, i.e. 4000 stands for the (4,0) and 3100 for the (2,0) resonance and sub–resonance, respectively. Part **a)**: only mean and uncertainty considered in b_4. For this case, the driving terms for the “resonance–free” lattice should be reduced compared with the nominal optics.
Part **b)**: all errors (mean, uncertainty and random corresponding to seed 2) considered in b_4.

[1)] Resonances have the same order than the multipoles by which they are driven while the order of sub–resonance is lower by a multiple of two (see Ref. [12] for details).

However, three other driving terms become slightly larger and one much larger. The reason could be that the dispersion suppressor cells are not exactly the same as the regular arc cells, which makes the "resonance–free" conditions not exactly satisfied.

Moreover Figure 6 **b)** shows that the cancellation of the driving terms is destroyed to a greater extent once the random errors are included, and in particular the (4,0) resonance driving term is increased. This comparison can explain why the strong 4^{th} order resonance still appears in the tune scan.

3.2 3^{rd} Order Resonances

A comparison of the 3^{rd} order resonance driving term excited along the ring has been done for the "resonance–free" lattice and for the nominal optics version 6 using the code SODD. To test more clearly the efficiency of the "resonance–free" lattice in suppressing the driving term, the b_3 spool pieces that are normally used to correct the sextupole components of the main dipoles are excluded. Unexpectedly, the "resonance–free" lattice is much worse than the nominal optics version 6 as shown in Figure 7. This problem can be ascribed to the chromaticity sextupoles which are present in only 23 cells rather than 25 cells in each arc as required for the "resonance–free" lattice [4]. Therefore 12 sextupoles were added in the dispersion suppressors (D.S.) to arrive at 25 cells with chromaticity sextupoles in each octant. As expected, we could achieve a large reduction of the 3^{rd} order resonance driving terms with this modification (see Figure 7).

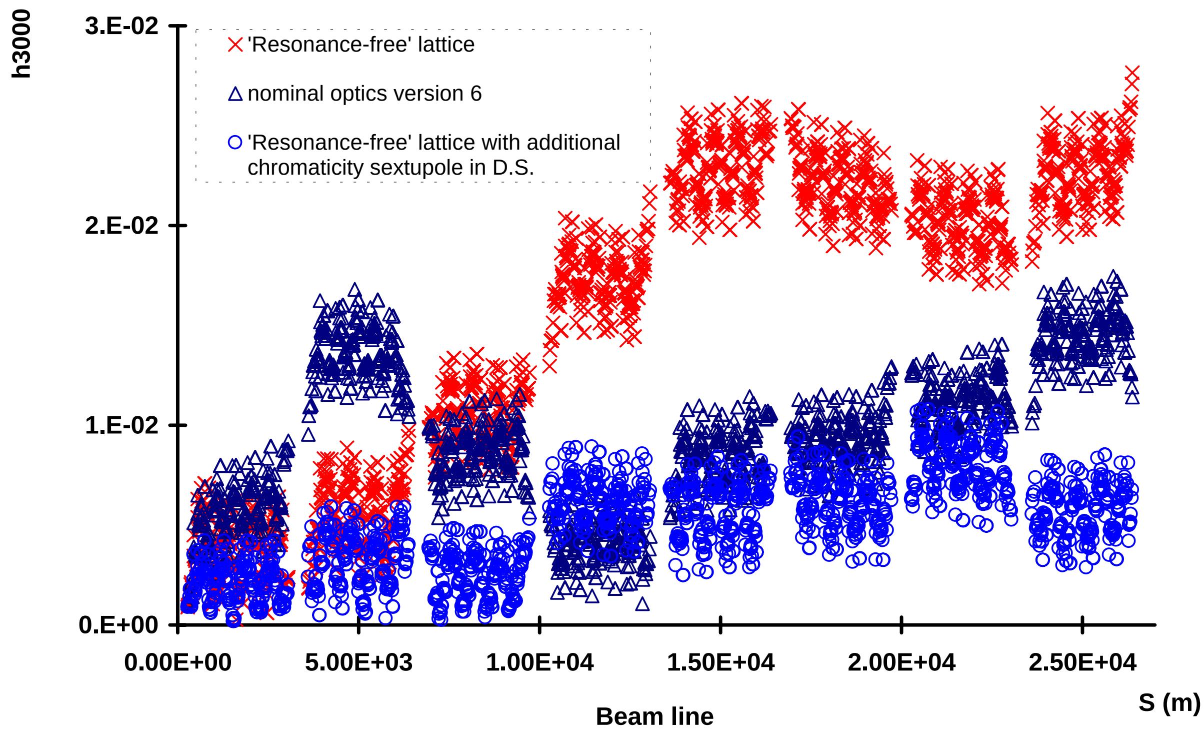

Figure 7: Comparison of the 3^{rd} order resonance driving term **h3000** (*random seed 1*) excited along the LHC ring for the "resonance–free" lattice and the nominal optics version 6 in the absence of b_3 spool pieces. The former is shown with and without extra chromaticity sextupoles in the D.S..

3.3 Long–Term Dynamic Aperture

Table 4 lists the long–term dynamic aperture for both the nominal optics version 6 and the "resonance–free" lattice, each lattice in four different configurations. From the comparison between the **Case A2** and **B2**, we know that the "resonance–free" lattice has a dynamic aperture much smaller in the case that the b_3 correction is excluded. This is consistent with the above analysis concerning the 3^{rd} order resonance driving term. In the case of additional chromaticity sextupoles added in the D.S. for the "resonance–free" lattice, even without b_3 correction the dynamic aperture has reached almost the same level as for the nominal optics version 6 with b_3 correction (compare **Case B4** and **A1** respectively). For the modified "resonance–free" lattice the b_3 correction is much less effective (compare **Case B4** with **B3** and **B1**). For the nominal optics version 6, we also have placed additional chromaticity sextupoles in the (D.S.). In this case the dynamic aperture becomes smaller without b_3 correction (compare **Case A4** with **A1**) while in the case with b_3 correction the dynamic aperture does not show any improvement (compare **Case A3** with **A1**).

Case	**Dynamic Aperture (100,000 turn)**			
	$\phi = 15°$		$\phi = 45°$	
	Minimum	**Average**	**Minimum**	**Average**
Case A1: Nominal optics v6	11.5	12.9	11.8	14.4
Case A2: **Case A1** without b_3 correction	10.7	12.5	10.0	12.7
Case A3: **Case A1** with additional Chro. Sext. in D.S. and b_3 correction	11.3	13.0	12.2	14.2
Case A4: **Case A1** with additional Chro. Sext. in D.S. and without b_3 correction	10.5	12.9	10.7	13.4
Case B1: "resonance–free" lattice	11.8	13.5	13.5	15.3
Case B2: **Case B1** without b_3 correction	8.1	9.7	8.2	10.3
Case B3: **Case B1** with additional Chro. Sext. in D.S. and b_3 correction	12.2	13.8	14.2	15.7
Case B4: **Case B1** with additional Chro. Sext. in D.S. and without b_3 correction	12.0	13.0	11.1	14.1

Table 4: Long–term dynamic aperture for the nominal LHC optics V6 and the "resonance–free" lattice with the error table **9901** at the nominal working point (0.28,0.31). Average and minimum value over 60 random seeds are given at the phase space angles $\phi = 15°, 45°$ respectively for each case.

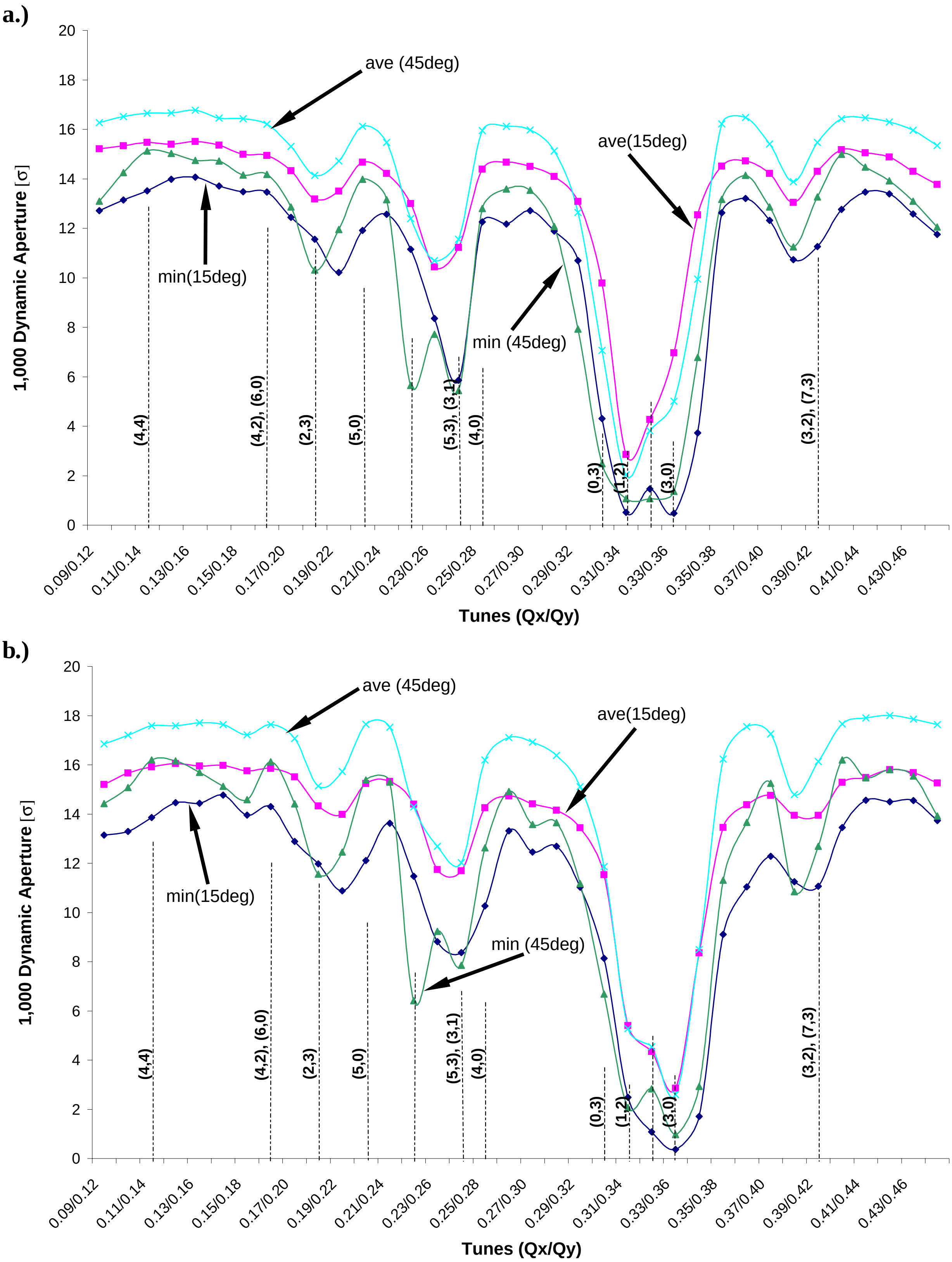

Figure 8: Short–term dynamic aperture (1,000 turns) v.s. tune for lattices with additional chromaticity sextupoles in the D.S. with the error table **9901**, but no b_3 spool piece correction. Average and minimum value over 60 random seeds are given at the phase space angles $\phi = 15°, 45°$ respectively for each pair of tunes, which are separated by 0.03.
Part **a)**: Nominal LHC lattice version 6;
Part **b)**: "Resonance–free" lattice.

In Figure 5 part b.) one finds the tunescan for the optimal **Case B3**, i.e. the "resonance–free" lattice with additional chromaticity sextupoles in the D.S. including the $\mathbf{b}_3$ correction. Far from strong low order resonances the dynamic aperture is slightly larger for all tune working points compared to **Case B1** (see part a.) of Figure 5. As mentioned before however, the real potential of this configuration is its tolerance against systematic field components including the b_3. It is interesting to note that the large dip in the dynamic aperture due to the 3^{rd} order resonances has not been improved much. We ascribe this to the fact that, although the first order contributions (in the multipole strength) to these resonances have been cancelled, the remaining higher order contribution are strong enough to keep the dynamic aperture small in this tune region.

Lastly, tunescans have been produced for the nominal LHC lattice version 6 and the "resonance–free" lattice, in both cases with the additional chromaticity sextupoles in the D.S. and without the b_3 spool piece correction, i.e. **Case A4** and **Case B4** respectively. Figure 8 part a.) and b.) shows these two tunescans. There is some apparent reduction for both cases compared to the situation including the b_3 spool piece correction, as seen in Figure 5. However, the "resonance–free" is much better behaved far from strong low order resonances. This fact becomes better visible (see Figure 9) when one depicts the ratio of the dynamic apertures of the two cases. For most pairs of tunes one finds an improvement between 5% and 10%, except where there are "valleys" due to the third and fourth order resonances, which appear at slightly shifted tunes for the two cases.

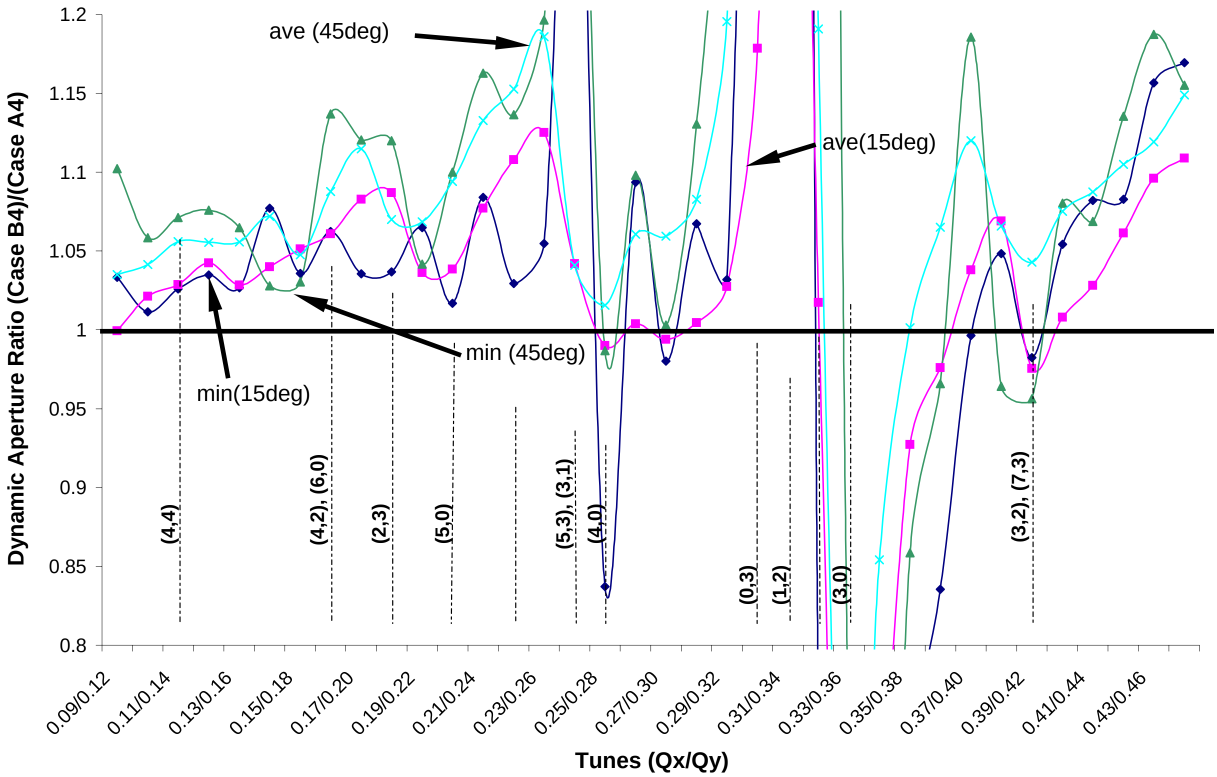

Figure 9: Ratio of short–term dynamic aperture (1,000 turns) (**Case B4**)/(**Case A4**) v.s. tune. Average and minimum ratio over 60 random seeds are given at the phase space angles $\phi = 15°, 45°$ respectively for each pair of tunes, which are separated by 0.03.

4 Conclusions

A thorough tune scan has been performed using three LHC models, namely the optics version 5 with the *target error table*, the nominal optics version 6 and the "resonance–free" lattice with the error table **9901**. Three stability islands have been found. In the stability island in which the nominal working point lies, the working point (0.27,0.30) was shown to be better, probably because it is further away from some dangerous 7^{th} order and 3^{rd} order resonances. All of these studies do not take into account linear imperfections and the beam–beam effect. The candidate working points for LHC according to the study of beam–beam effects [13] seem to have a fairly acceptable dynamic aperture [1]. Globally, the nominal optics version 6 is favourable to get larger dynamic aperture in those stability islands compared with the optics version 5.

For the "resonance–free" lattice, the tune scan shows that stability islands are still separated by the 3^{rd} and 4^{th} order resonances. However, the dynamic aperture for this lattice is improved, although not very significantly. The efficiency in suppressing the 4^{th} order resonance driving terms might be affected to some extent by the irregular cells of the D.S. and the random errors in $\mathbf{b}_4$. Additional chromaticity sextupoles in the D.S. are necessary to cancel the contribution to the 3^{rd} order resonance driving terms from all chromaticity sextupoles in each arc. For this modified "resonance–free" lattice, the b_3 spool pieces correction system is much less needed, or alternatively it allows for potentially larger systematic $\mathbf{b}_3$ errors.

Acknowledgements

One of the authors (L.J.) would like to thank J. Gareyte for his invitation and his support. The help from J.–P. Koutchouk with the use of the error table and suggestions are acknowledged. Thanks also go to H. Grote for his help with some software and the use of computers, Y. Papaphilippou for his help with the use of GRR code and A. Verdier for helpful discussions concerning the "resonance–free" lattice.

References

[1] L. Jin and F. Schmidt, " Dynamic Aperture Tune Scan for LHC Version 5 at Injection Energy", LHC Project Note 182 (1999).

[2] F. Schmidt *et al.*, "Improvement of LHC Dynamic Aperture via Octupole Spool Pieces for the Nominal tunes", LHC Project Report 253 (1998).

[3] F. Schmidt, "SixTrack, version 1.2, Single Particle Tracking Code treating Transverse Motion with Synchrotron Oscillations in a Symplectic Manner", CERN SL/94–56(AP) (1994).

[4] A. Verdier, "Resonance free lattices for A.G. machines", 1999 Particle Accelerator Conference New York City, NY, USA, CERN–SL-99–018 AP.

[5] F. Schmidt and A. Verdier, "Optimisation of the LHC Dynamic Aperture via the Phase Advance of the Arc Cells", LHC Project Report 297 (1999).

[6] J.–P. Koutchouk, "The LHC Dynamic Aperture", LHC Project Report 296 (1999).

[7] J. Laskar, "Secular terms of classical planetary theories using the results of general theory", Astron. Astrophys. **198** 341–362 (1988).

[8] Y. Papaphilippou, "Frequency Maps of LHC Models", LHC Project Report 299 (1999).

[9] Y. Papaphilippou and F. Schmidt, "Normal Form Approaches and Resonance Analysis of LHC Models", LHC Project Report 255 (1998).

[10] E. Forest, "The Code Dalie" (unpublished) (1986).

[11] F. Schmidt, "SODD: A Computer Code to calculate Detuning and Distortion Function Terms in First and Second Order", CERN SL/Note 99–009 (AP) (1999).

[12] A. Schoch, "Theory of linear and non–linear perturbations of betatron oscillations in alternating gradient synchrotrons", CERN 57–21, (1958).
[13] J. Gareyte, "Beam–Beam Design criteria for LHC", in proceedings of the Workshop on Beam–Beam effects in Large Hadron Colliders, CERN, Geneva, 1999, edited by J. Poole and F. Zimmermann, CERN–SL–99–039–AP.

Appendix A: Error Tables

Target Error Table						
(Persistent & Geometric)						
Order	**Mean**		**Uncertainty**		**Random**	
n	**b**	**a**	**b**	**a**	**b**	**a**
3	-11.07		2.38	0.29	1.45	0.43
4			0.069	0.139	0.49	0.49
5	0.376		0.122	0.376	0.65	0.334
6			0.057	0.057	0.28	0.14
7	-0.094		0.023		0.25	0.25
8					0.21	0.22
9	0.347		0.081		0.22	0.29
10					0.24	0.24
11	0.585				0.20	0.20
Error Table 9901						
(Persistent & Geometric)						
Order	**Mean**		**Uncertainty**		**Random**	
n	**b**	**a**	**b**	**a**	**b**	**a**
3	-9.7005	-0.082	1.376	0.867	1.474	0.479
4	0.2234		0.344	0.130	0.513	0.513
5	0.8874	0.007	0.436	0.418	0.428	0.341
6	-0.0106		0.057	0.057	0.088	0.165
7	-0.1584	0.017	0.053		0.219	0.078
8	-0.0003				0.043	0.084
9	0.3618	-0.006	0.028		0.071	0.115
10						0.012
11	0.5672	0.002				

Table 5: The Multipole components of the main LHC dipoles at injection energy. Unit: 10^{-4} relative field error at a radius of 17 mm.